OCEAN TURBULENCE

W.D. Smyth & J.N. Moum

College of Oceanic & Atmospheric Sciences
Oregon State University
Corvallis, OR 97330

This is an extended version of "3D Turbulence", an article written for
Academic Press Encyclopedia of Ocean Sciences

Last revised September, 2000

Table of Contents

1. INTRODUCTION

This article describes fluid turbulence with application to the Earth's oceans. We begin with the simple, classical picture of stationary, homogeneous, isotropic turbulence. We then discuss departures from this idealized state that occur in small-scale geophysical flows. The article closes with a tour of some of the many physical regimes in which ocean turbulence has been observed, and a brief discussion of numerical modeling.

Turbulent flow has been a source of fascination for centuries. The term "turbulence" appears to have been used first in reference to fluid flows by da Vinci, who studied the phenomenon extensively. Today, turbulence is frequently characterized as the last great unsolved problem of classical physics. It plays a

central role in both engineering and geophysical fluid flows. Its study led to the discovery of the first strange attractor by Lorenz in 1963, and thus to the modern science of chaotic dynamics. In the past few decades, tremendous insight into the physics of turbulence has been gained through theoretical and laboratory study, geophysical observations, improved experimental techniques and computer simulations.

Turbulence results from the nonlinear nature of advection, which enables interaction between motions on different spatial scales. Consequently, an initial disturbance with a given characteristic length scale tends to spread to progressively larger and smaller scales. The simplest example of this is a one-dimensional disturbance consisting of a single Fourier component $u = \sin(kx)$, subjected to the advection operation $u_t = -uu_x$ (where subscripts denote partial derivatives). The advection operation introduces a new Fourier component with wavenumber $2k$. More generally, advection of a disturbance with wavenumber k by a second disturbance with wavenumber l introduces two new components with wavenumbers $k+l$ and $k-l$. In real turbulence, this expansion of the spectral range is limited at large scales by boundaries and/or body forces, at small scales by viscosity. If the range of scales becomes sufficiently large, the flow takes a highly complex form whose details defy prediction.

The roles played by turbulence in the atmosphere and oceans can be classified into two categories: momentum transport and scalar mixing. In transporting momentum, turbulent motions behave in a manner roughly analogous to molecular viscosity, reducing differences in velocity between different regions of a flow. For example, winds transfer momentum to the Earth via strong turbulence in the planetary boundary layer (a kilometer-thick layer adjacent to the ground) and are thus decelerated.

Scalar mixing refers to the homogenization of fluid properties such as temperature by random molecular motions. Molecular mixing rates are proportional to spatial gradients, which are greatly amplified due to the stretching and kneading (i.e. stirring) of fluid parcels by turbulence. This process is illustrated in figure 1, which shows the evolution of an initially circular region of dyed fluid in a numerical simulation. Under the action of molecular mixing (or diffusion) alone, an annular region of intermediate shade gradually expands as the dyed fluid mixes with the surrounding fluid. If the flow is turbulent, the result is dramatically different. The circle is distended into a highly complex shape, and the region of mixed fluid expands rapidly.


Figure 1: A comparison of mixing enhanced by turbulence with mixing due to molecular processes alone, as revealed by a numerical solution of the equations of motion. The initial state includes a circular region of dyed fluid in a white background. Two possible evolutions are shown: one in which the fluid is motionless (save for random molecular motions), and one in which the fluid is in a state of fully developed, two-dimensional turbulence. The mixed region (yellow-green) expands much more rapidly in the turbulent case.
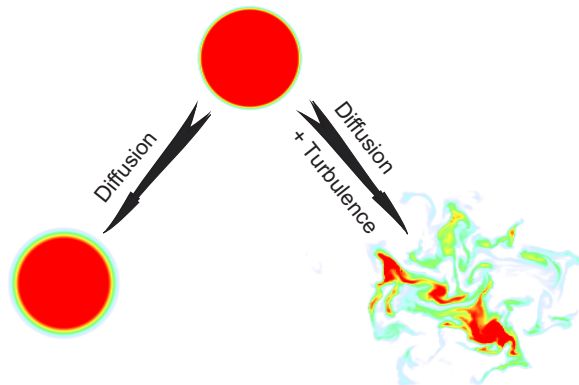
2. THE MECHANICS OF TURBULENCE

We now describe the main physical mechanisms that drive turbulence at the smallest scales. The description is presented in terms of **strain** and **vorticity**, quantities that represent the tendency of the flow at any point to deform and to rotate fluid parcels, respectively (figure 2). A major and recent insight is that vorticity and strain are not distributed randomly in turbulent flow, but rather are concentrated into coherent regions, each of which is dominated by one type of motion or the other.

Figure 2: Schematic representations of vorticity and strain, in terms of the effect they have on an initially circular fluid parcel in two-dimensional flow. Vorticity rotates the parcel without changing its shape. Strain stretches the parcel in one direction and compresses it in the orthogonal direction (to conserve mass). Flow in the neighborhood of a point following the motion can always be decomposed into a vortical component and a strain component. In three dimensions the geometry is more complex, but the concepts are the same.
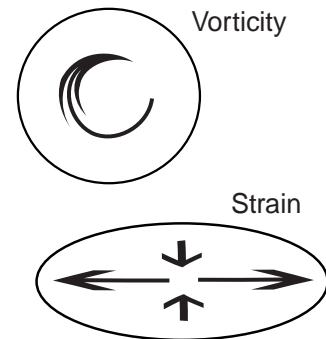
The first mechanism we consider is **vortex rollup** due to shear instability (figure 3). This process results in a vorticity concentration of dimension close to unity, i.e. a line vortex. Line vortices are reinforced by the process of **vortex stretching**. When a vortex is stretched by the surrounding flow, its rotation rate increases to conserve angular momentum. Opposing these processes is molecular **viscosity**, which both dissipates vorticity and fluxes it away from strongly rotational regions.
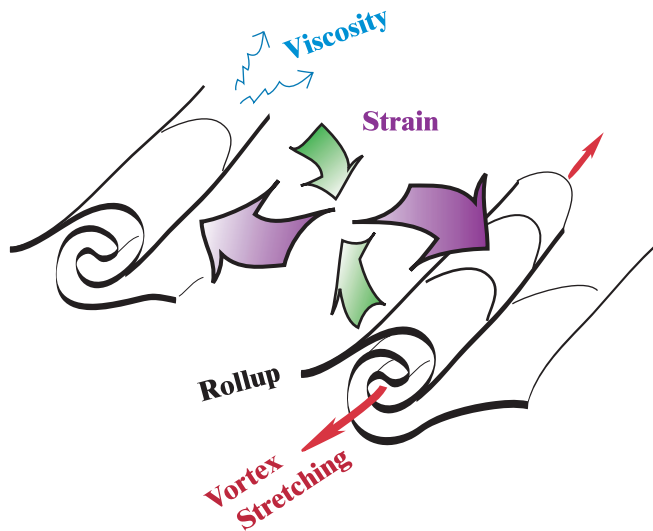
Figure 3: Schematic illustration of line vortices and strained regions in turbulent flow. Fluid parcels in the vortex interiors rotate with only weak deformation. In contrast, fluid parcels moving between the vortices are rapidly elongated in the direction of the purple arrows and compressed in the direction of the green arrows.
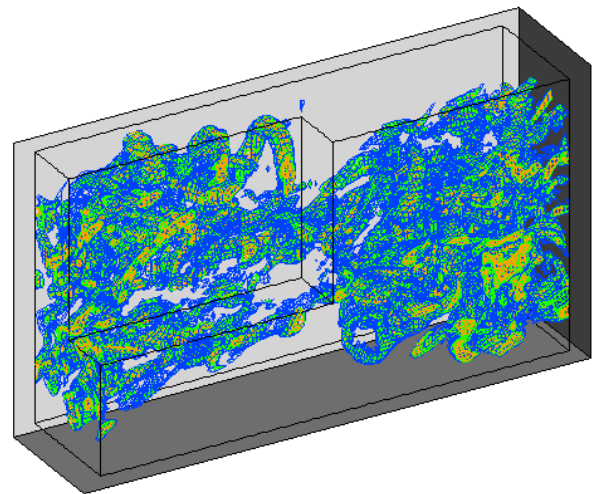
Figure 4: Computer simulation of turbulence as it is believed to occur in the ocean thermocline. The colored meshes indicate surfaces of constant vorticity.

Turbulence may thus be visualized as a loosely tangled "spaghetti" of line vortices, which continuously advect each other in complex ways (figure 4). At any given time, some vortices are being created via rollup, some are growing due to vortex stretching, and some are decaying due to viscosity. Many, however, are in a state of approximate equilibrium among these processes, so that they appear as long-lived, coherent features of the flow. Mixing is not accomplished within the vortices themselves; in fact, these regions are relatively stable, like the eye of a hurricane. Instead, mixing occurs mainly in regions of intense **strain** that exist between any two nearby vortices that rotate in the same sense (figure 3). It is in these regions that fluid parcels are deformed to produce amplified gradients and consequent rapid mixing.

3. STATIONARY, HOMOGENEOUS, ISOTROPIC TURBULENCE

Although the essential structures of turbulence are not complex (figure 3), they combine in a bewildering range of sizes and orientations that defies analysis (figure 4). Because of this, turbulence is most usefully understood in statistical terms. Although the statistical approach precludes detailed prediction of flow evolution, it does give access to the rates of mixing and property transport, which are of primary importance in most applications. Statistical analyses focus on the various moments of the flow field, defined with respect to some averaging operation. The average may be taken over space and/or time, or it may be an ensemble average taken over many flows begun with similar initial conditions.
Analyses are often simplified using three standard assumptions. The flow statistics are assumed to be

- stationary (invariant with respect to translations in time),
- homogeneous (invariant with respect to translations in space), and/or
- isotropic (invariant with respect to rotations).

Much of our present understanding pertains to this highly idealized case. Our description will focus on the power spectra that describe spatial variability of kinetic energy and scalar variance. The spectra provide insight into the physical processes that govern motion and mixing at different spatial scales.

3.1 Velocity fields

Big whorls have little whorls
That feed on their velocity
And little whorls have lesser whorls
And so on to viscosity
L.F. Richardson (1922)

Suppose that turbulence is generated by a steady, homogenous, isotropic stirring force whose spatial variability is described by the Fourier wavenumber k_F. Suppose further that the turbulence is allowed to

evolve until equilibrium is reached between forcing and viscous dissipation, i.e. the turbulence is statistically stationary.

Figure 5 shows typical wavenumber spectra of kinetic energy, $E(k)$, and kinetic energy dissipation, $D(k)$, for such a flow. $E(k)dk$ is the kinetic energy contained in motions whose wavenumber magnitudes lie in an interval of width dk surrounding k. $D(k)dk = \nu k^2 E(k)dk$ is the rate at which that kinetic energy is dissipated by molecular viscosity (ν) in that wavenumber band. The net rate of energy dissipation is given by $\varepsilon = \int\limits_0^\infty D(k)dk$, and is equal (in the equilibrium state) to the rate at which energy is supplied by the stirring force.

Nonlinear interactions induce a spectral flux, or cascade, of energy. The energy cascade is directed primarily (though not entirely) toward smaller scales, i.e. large-scale motions interact to create smaller-scale motions. The resulting small eddies involve sharp velocity gradients, and are therefore susceptible to viscous dissipation. Thus, while kinetic energy resides mostly in large-scale motions, it is dissipated primarily by small-scale motions. (Note that the logarithmic axes used in figure 5 tend to de-emphasize the peaks in the energy and dissipation rate spectra.) Turbulence can be envisioned as a "pipeline" conducting kinetic energy through wavenumber space: in at the large scales, down the spectrum, and out again at the small scales, all at a rate ε. The cascade concept was first suggested early in the 20th century by L.F. Richardson, who immortalized his idea in the verse quoted at the beginning of this section.

The energy spectrum is often divided conceptually into three sections. The **energy-containing subrange** encompasses the largest scales of motion, while the **dissipation subrange** includes the smallest scales. If the range of scales is large enough, there may exist an intermediate range in which the form of the spectrum is independent of both large-scale forcing and small-scale viscous effects. This intermediate range is called the **inertial subrange**. The existence of the inertial subrange depends on the value of the **Reynolds number**: $\mathrm{Re} = u\ell/\nu$, where u and ℓ are scales of velocity and length characterizing the energy-containing range. The spectral distance between the energy-containing subrange and the dissipation subrange, k_F / k_K, is proportional to $\mathrm{Re}^{3/4}$. A true inertial subrange exists only in the limit of large Re.

energy   /   inertial   /   dissipation

Figure 5: Theoretical wavenumber spectra of kinetic energy and kinetic energy dissipation for stationary, homogeneous, isotropic turbulence forced at wavenumber k_F . Approximate locations of the energy containing, inertial, and dissipation subranges are indicated, along with the Kolmogorov wavenumber k_K . Axes are logarithmic. Numerical values depend on Re and are omitted here for clarity.
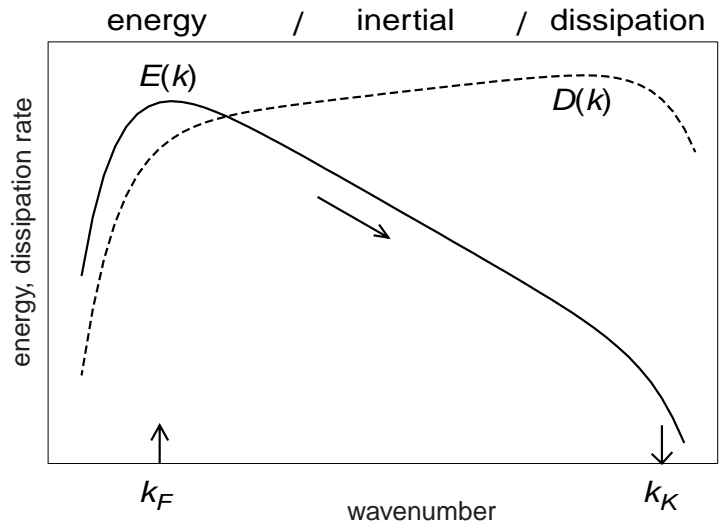
In the 1940s, the Russian statistician A.N. Kolmogorov hypothesized that, in the limit $\mathrm{Re} \rightarrow \infty$, the distribution of eddy sizes in the inertial and dissipation ranges should depend on only two parameters (besides wavenumber): the dissipation rate ε and the viscosity v , i.e. $E = E(k;\varepsilon,v)$. Dimensional reasoning then implies that $E = \varepsilon^{1/4} v^{5/4} f\left(k/k_K\right)$, where $k_K = (\varepsilon/v^3)^{1/4}$ is the Kolmogorov wavenumber and f is some universal function. Thus, with the assumptions of stationarity, homogeneity, isotropy and infinite Reynolds number, all types of turbulence, from flow over a wing to convection in the interior of the Sun, appear as manifestations of a single process whose form depends only on the viscosity of the fluid and the rate at which energy is transferred through the "pipeline". This tremendous simplification is generally regarded as the beginning of the modern era of turbulence theory.

Kolmogorov went on to suggest that the spectrum in the inertial range should be simpler still by virtue of being independent of viscosity. In that case $E = E(k,\varepsilon)$, and the function can be predicted from dimensional reasoning alone up to the universal constant C_K , *viz.* $E = C_K \varepsilon^{2/3} k^{-5/3}$. This power-law spectral form indicates that motions in the inertial subrange are *self-similar,* i.e. their geometry is invariant under coordinate dilations.

Early efforts to identify the inertial subrange in laboratory flows were inconclusive because the Reynolds number could not be made large enough. (In a typical, laboratory-scale water channel, $u \sim 0.1 m/s,\ \ell \sim 0.1m,$ and $v \sim 10^{-6} m^2/s$, giving $\mathrm{Re} \sim 10^4$. In a typical wind tunnel, $u \sim 1 m/s,\ \ell \sim 1m,$ and $v \sim 10^{-5} m^2/s$, so that $\mathrm{Re} \sim 10^5$.) The inertial subrange spectrum was first verified in 1962 using measurements in a strongly turbulent tidal channel near Vancouver Island, where typical turbulent velocity scales $u \sim 1 m/s$ and length scales $\ell \sim 100m$ combine with the kinematic viscosity of seawater $v \sim 10^{-6} m^2/s$ to produce a Reynolds number $\mathrm{Re} \sim 10^8$. From this experiment and others like it, the value of C_K has been determined to be near 1.6.

3.2 Passive scalars and mixing

Now let us suppose that the fluid possesses some scalar property θ, such as temperature or the concentration of some chemical species, and that the scalar is dynamically *passive*, i.e. its presence does not affect the flow[1]. Suppose also that there is a source of large-scale variations in θ, e.g. an ambient temperature gradient in the ocean. Isosurfaces of θ will be folded and kneaded by the turbulence so that their surface area tends to increase. As a result, typical gradients of θ will also increase, and will become susceptible to erosion by molecular diffusion. Scalar variance is destroyed at a rate χ , which is equal (in equilibrium) to the rate at which variance is produced by the large eddies.

Thus, the turbulent mixing of the scalar proceeds in a manner similar to the energy cascade discussed above. However, there is an important difference in the two phenomena. Unlike energy, scalar variance is driven to small scales by a combination of two processes. First, scalar gradients are compressed by the strain fields between the turbulent eddies. Second, the eddies themselves are continually redistributed toward smaller scales. (The latter process is just the energy cascade described in the previous section).

Figure 6 shows the equilibrium scalar variance spectrum for the case of heat mixing in water. Most of the variance is contained in the large scales, which are separated from the small scales by an **inertial-convective subrange** (so called because temperature variance is convected by motions in the inertial subrange of the energy spectrum). Here, the spectrum depends only on ε and χ ; its form is

$E_\theta = \beta \chi \varepsilon^{-1/3} k^{-5/3}$, where β is a universal constant.

Figure 6: Theoretical wavenumber spectra of scalar variance and dissipation for stationary, homogeneous, isotropic turbulence forced at wavenumber k_F . Approximate locations of the variance-containing, inertial-convective, viscous-convective, and viscous-diffusive subranges are indicated, along with the Kolmogorov wavenumber k_K and the Batchelor wavenumber k_B . Axes are logarithmic. Numerical values depend on Re and are omitted here for clarity.
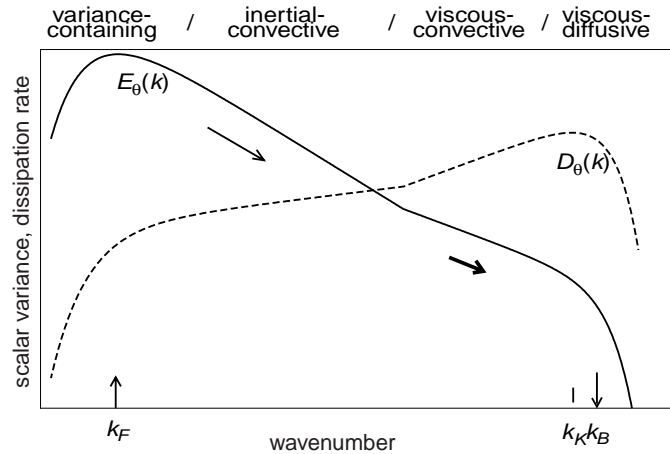
The shape of the spectrum at small scales is very different from that of the energy spectrum, owing to the fact that, in seawater, the molecular diffusivity, κ, of heat is smaller than the kinematic viscosity. The ratio of viscosity to thermal diffusivity is termed the Prandtl number (i.e. $\Pr = v / \kappa$) and has a value near 7 for seawater. In the **viscous-convective subrange**, the downscale cascade of temperature variance is slowed because the eddies driving the cascade are weakened by viscosity. In other words, the first of the two processes listed above as driving the scalar variance cascade is no longer active. There is no

---

[1] In the case of temperature, this is true only for sufficiently small-scale fluctuations; see *Buoyancy Effects* for details.

corresponding weakening of temperature gradients, because molecular diffusivity is not active on these scales. As a result, there is a tendency for variance to "accumulate" in this region of the spectrum and the spectral slope is reduced from $-5/3$ to -1. However, the variance in this range is ultimately driven into the **viscous-diffusive subrange**, where it is finally dissipated by molecular diffusion. A measure of the wavenumber at which scalar variance is dissipated is the Batchelor wavenumber, $k_B = (\varepsilon / \nu \kappa^2)^{1/4}$. When Pr>1, as for seawater, the Batchelor wavenumber is larger than the Kolmogorov wavenumber, i.e. temperature fluctuations can exist at smaller scales than velocity fluctuations.

In summary, the energy and temperature spectra exhibit many similarities. Energy (temperature variance) is input at large scales, cascaded down the spectrum by inertial (convective) processes, and finally dissipated by molecular viscosity (diffusion). The main difference between the two spectra is the viscous-convective range of the temperature spectrum, in which molecular smoothing acts on the velocity field but not on the temperature field. This difference is even more pronounced if the scalar field represents salinity rather than temperature, for salinity is diffused even more weakly than heat. The ratio of the molecular diffusivities of heat and salt is of order 10^2, so that the smallest scales of salinity fluctuation in seawater are ten times smaller than those of temperature fluctuations.

4. TURBULENCE IN GEOPHYSICAL FLOWS

The assumptions of homogeneity, stationarity and isotropy as employed by Kolmogorov have permitted tremendous advances in our understanding of turbulence. In addition, approximations based on these assumptions are used routinely in all areas of turbulence research. However, we must ultimately confront the fact that physical flows rarely conform to our simplifying assumptions. In geophysical turbulence, symmetries are upset by a complex interplay of effects. Here, we focus on three important classes of phenomena that modify small-scale turbulence in the ocean: shear, stratification and boundary proximity.

4.1 Shear Effects

Geophysical turbulence often occurs in the presence of a current which varies on scales much larger than the energy-containing scales of the turbulence, and evolves much more slowly than the turbulence. Examples include atmospheric jet streams and large-scale ocean currents such as the Gulf Stream and the Equatorial Undercurrent. In such cases, it makes sense to think of the background current as an entity separate from the turbulent component of the flow.

Shear upsets homogeneity and isotropy by deforming turbulent eddies. By virtue of the resulting anisotropy, turbulent eddies exchange energy with the background shear through the mechanism of Reynolds stresses. Reynolds stresses represent correlations between velocity components parallel to and perpendicular to the background flow, correlations that would vanish if the turbulence were isotropic. Physically, they represent transport of momentum by the turbulence. If the transport is directed counter to

the shear, kinetic energy is transferred from the background flow to the disturbance. This energy transfer is one of the most common generation mechanisms for geophysical turbulence.

The simplest example of shear-amplified vortices is the Kelvin-Helmholtz instability shown in figure 7a. The vortex rollup process shown in figure 3 is closely related to this instability. A more complex example is the sinuous instability of a jet (figure 7b). This structure may be thought of in an approximate sense as two interacting trains of Kelvin-Helmholtz billows. Sinuous instability is partly responsible for the hot and cold core rings of the Gulf Stream.
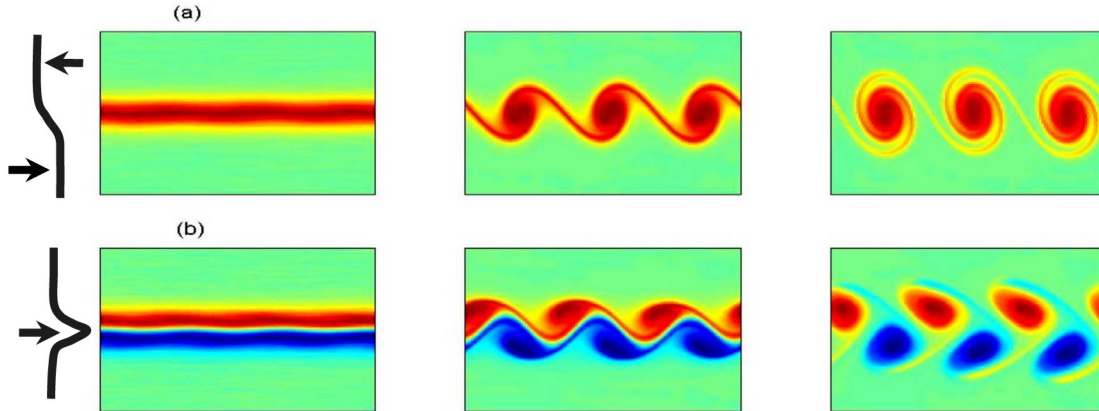
Figure 7: Two common examples of vortex generation via shear instability in a two-dimensional model flow. Schematics at the left indicate the initial velocity profiles. Colors indicate vorticity (blue=clockwise; red=counterclockwise).

In sheared turbulence, the background shear acts primarily on the largest eddies. Motions on scales much smaller than the Corrsin scale, $L_C = \sqrt{\varepsilon / S^3}$ (where $S = dU / dz$, the vertical gradient of the ambient horizontal current) are largely unaffected.

4.2 Buoyancy Effects

Most geophysical flows are affected to some degree by buoyancy forces, which arise due to spatial variations in density. Buoyancy breaks the symmetry of the flow by favoring the direction in which the gravitational force acts. Buoyancy effects can either force or damp turbulence. Forcing occurs in the case of **unstable** density stratification, i.e. when heavy fluid overlies light fluid. This happens in the atmosphere on warm days, when the air is heated from below. The resulting turbulence is often made visible by cumulus clouds. In the ocean, surface cooling (at night) has a similar effect. Unstable stratification in the ocean can also result from evaporation, which increases surface salinity and hence surface density. In each of these cases, unstable stratification results in convective turbulence, which can be extremely vigorous. Convective turbulence usually restores the fluid to a stable state soon after the destabilizing flux ceases (e.g. when the sun rises over the ocean).

Buoyancy effects tend to damp turbulence in the case of **stable** stratification, i.e. when light fluid overlies heavier fluid. In stable stratification, a fluid parcel displaced from equilibrium oscillates vertically with frequency $N = \sqrt{-g\,\rho^{-1}d\rho/dz}$, the buoyancy or **Brunt-Vaisala frequency** (g represents acceleration due to gravity and $\rho(z)$ is the ambient mass density). A result of stable stratification that can dramatically alter the physics of turbulence is the presence of **internal gravity waves** (IGW). These are similar to the more familiar interfacial waves that occur at the surfaces of oceans and lakes, but continuous density variation adds the possibility of vertical propagation. Visible manifestations of IGW included banded clouds in the atmosphere and slicks on the ocean surface. IGW carry momentum, but no scalar flux and no vorticity.

In **strongly stable stratification**, motions may be visualized approximately as two-dimensional turbulence (figure 1) flowing on nearly horizontal surfaces that undulate with the passage of IGW. The quasi-two-dimensional mode of motion carries all of the vorticity of the flow (since IGW carry none), and is therefore called the **vortical mode**.

In **moderately stable stratification**, three-dimensional turbulence is possible, but its structure is modified by the buoyancy force, particularly at large scales. Besides producing anisotropy, the suppression of vertical motion damps the transfer of energy from any background shear, thus reducing the intensity of turbulence. On scales much smaller than the Ozmidov scale, $L_O = \sqrt{\varepsilon/N^3}$, buoyancy has only a minor effect[2]. The relative importance of stratification and shear depends on the magnitudes of S and N. If $S \gg N$, shear dominates and turbulence is amplified. On the other hand, if $S \ll N$, the buoyancy forces dominate and turbulence is suppressed. The simulated turbulence shown in figure 4 developed from Kelvin-Helmholtz instability (figure 7a) of a stratified shear layer in which $S \gg N$.

The relationship between IGW and turbulence in stratified flow is exceedingly complex. At scales in excess of a few meters (figure 8), ocean current fluctuations behave like IGW, displaying the characteristic spectral slope k^{-2}. At scales smaller than the Ozmidov scale (typically a few tens of cm), fluctuations differ little from the classical picture of homogeneous, isotropic turbulence. The intermediate regime is a murky mix of nonlinear IGW and anisotropic turbulence that is not well understood at present.

The breaking of IGW is thought to be the major source of turbulence in the ocean interior. Breaking occurs when a superposition of IGW generates locally strong shear and/or weak stratification. IGW propagating obliquely in a background shear may break upon encountering a **critical level**, a depth at which the background flow speed equals the horizontal component of the wave's phase velocity[3]. Just as waves may generate turbulence, turbulent motions in stratified flow may radiate energy in the form of waves.

---

[2] In *Passive Scalars and Mixing*, we used temperature as an example of a dynamically passive quantity. This approximation is valid only on scales smaller than the Ozmidov scale.
[3] Many dramatic phenomena occur where wave speed matches flow speed. Other examples include the hydraulic jump and the sonic boom.

Figure 8: Energy spectrum (cf. figure 5) extended to larger scales to include IGW plus anisotropic stratified turbulence. Labels represent approximate length scales from ocean observations. Axes are logarithmic.
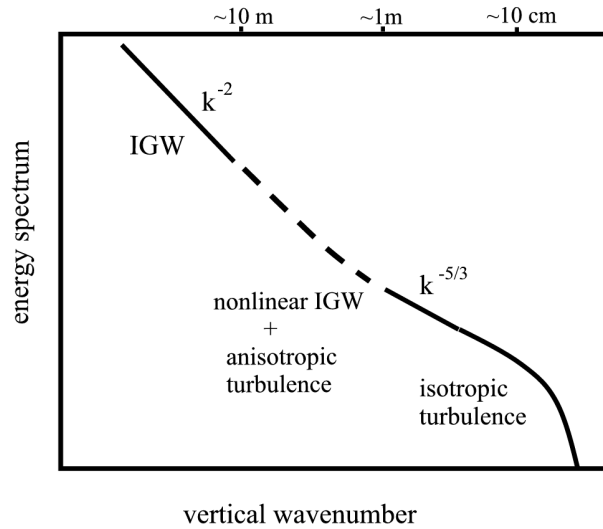
In stably stratified turbulence, the distinction between **stirring** and **mixing** of scalar properties becomes crucial. Stirring refers to the advection and deformation of fluid parcels by turbulent motion, while mixing involves actual changes in the scalar properties of fluid parcels. Mixing can only be accomplished by molecular diffusion, though it is accelerated greatly in turbulent flow due to stirring (cf. figure 1 and the accompanying discussion). In stable stratification, changes in the density field due to stirring are **reversible**, i.e. they can be undone by gravity. In contrast, mixing is **irreversible**, and thus leads to a permanent change in the properties of the fluid. For example, consider a blob of water that has been warmed at the ocean surface, then carried downward by turbulent motions. If the blob is *mixed* with the surrounding water, its heat will remain in the ocean interior, whereas if the blob is only *stirred*, it will eventually bob back up to the surface and return its heat to the atmosphere.

4.3 Boundary Effects

It is becoming increasingly clear that most turbulent mixing in the ocean takes place near boundaries, either the solid boundary at the ocean bottom, or the moving boundary at the surface. All boundaries tend to suppress motions perpendicular to themselves, thus upsetting both the homogeneity and the isotropy of the turbulence. Solid boundaries also suppress motion in the tangential directions. Therefore, since the velocity must change from zero at the boundary to some nonzero value in the interior, a shear is set up, leading to the formation of a turbulent boundary layer. Turbulent boundary layers are analogous to viscous boundary layers, and are sites of intense, shear-driven mixing (figure 9). In turbulent boundary layers, the characteristic size of the largest eddies is proportional to the distance from the boundary.

Near the ocean surface, the flexible nature of the boundaries leads to a multitude of interesting phenomena, notably surface gravity waves and Langmuir cells. These phenomena contribute significantly to upper-ocean mixing and thus to air-sea fluxes of momentum, heat and various chemical species. Boundaries also include obstacles to the flow, such as islands and seamounts, which create turbulence. If flow over an obstacle is stably stratified, buoyancy-accelerated bottom flow and a downstream hydraulic jump may drive turbulence (figure 9).

Figure 9: Flow over Stonewall bank, on the continental shelf off the Oregon coast. Colors show the kinetic energy dissipation rate, with red indicating strong turbulence. White contours are isopycnals, showing the effect of density variations in driving the downslope flow. Three distinct turbulence regimes are visible: (**1**) turbulence driven by shear at the top of the rapidly moving lower layer, (**2**) a turbulent bottom boundary layer and (**3**) a hydraulic jump.
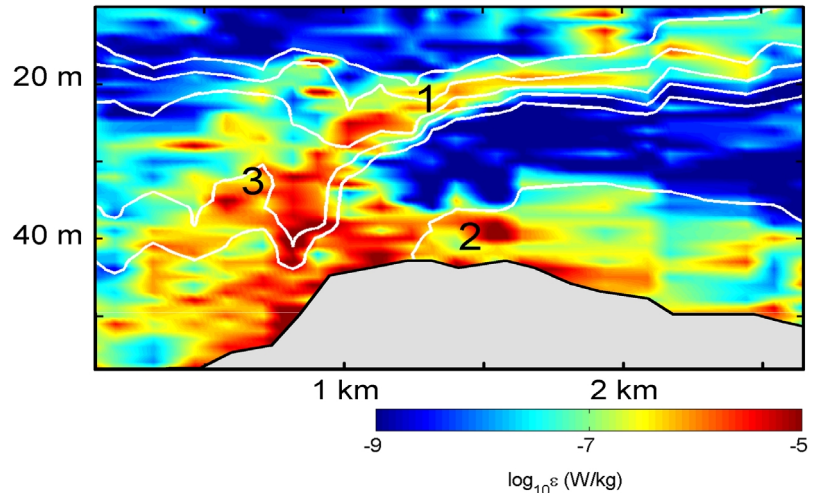
Ocean turbulence is often influenced by combinations of shear, stratification and boundary effects. In the example shown in figure 9, all three effects combine to create an intensely turbulent flow that diverges dramatically from the classical picture of stationary, homogeneous, isotropic turbulence.
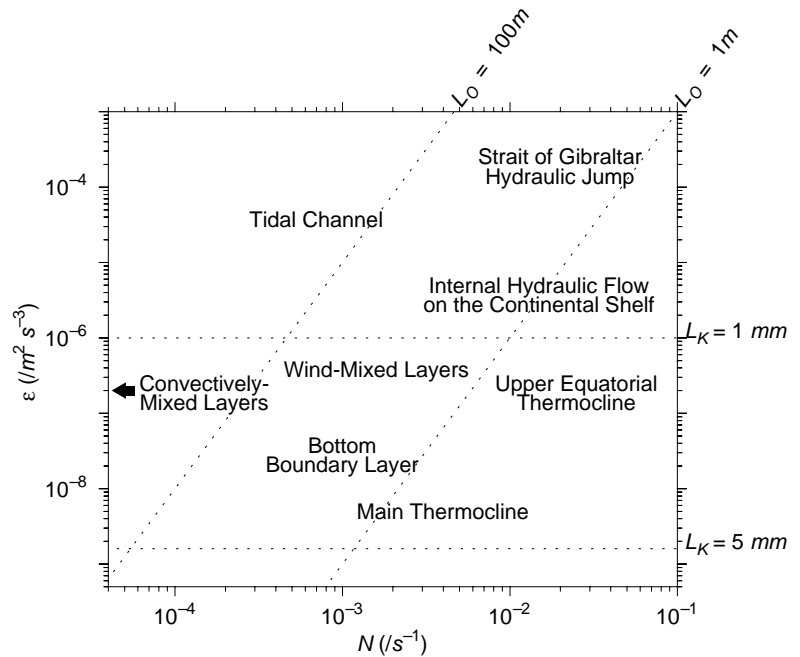
5. LENGTH SCALES OF OCEAN TURBULENCE

Examples of turbulent flow regimes that have been observed in the ocean can be considered in terms of typical values of ε and N that pertain to each (Figure 10). This provides the information to estimate both largest and smallest scales present in the flow. The largest scale is approximated by the Ozmidov scale, which varies from a few cm in the ocean's thermocline to several hundred meters in weakly stratified and/or highly energetic flows. The smallest scale, the Kolmogorov scale $L_K = k_K^{-1}$, is typically 1cm or less.

Turbulence in the **upper ocean mixed layer** may be driven by wind and/or by convection due to surface cooling. In the convectively mixed layer, N is effectively zero within the turbulent region, and the maximum length scale is determined by the depth of the mixed layer. In both cases the free surface limits length scale growth.

Turbulence in the **upper equatorial thermocline** is enhanced by the presence of shear associated with the strong equatorial zonal current system. Stratification tends to be considerably stronger in the upper thermocline than in the main thermocline. Despite weak stratification, turbulence in the **main thermocline** tends to be relatively weak due to isolation from strong forcing. Turbulence in this region is generated primarily by IGW interactions.

Figure 10: Regimes of ocean turbulence located with respect to stratification and energy dissipation. Dotted lines indicate Ozmidov and Kolmogorov length scales.

Tidal channels are sites of extremely intense turbulence, forced by interactions between strong tidal currents and three-dimensional topography. Length scales are limited by the geometry of the channel. Turbulent length scales in the **bottom boundary layer** are limited below by the solid boundary and above by stratification. Intense turbulence is also found in **hydraulically controlled flows**, such as have been found in the Strait of Gibraltar, and also over topography on the continental shelf (cf. Figure 9). In these flows the stratification represents a potential energy supply that drives strongly sheared downslope currents, the kinetic energy of which is in turn converted to turbulence and mixing.

All of these turbulence regimes are subjects of ongoing observational and theoretical research, aimed at generalized Kolmogorov's view of turbulence to encompass the complexity of real geophysical flows.


6. MODELING OCEAN TURBULENCE

A measure of our understanding of any phenomenon is our ability to model it. Besides providing a predictive capability, models of ocean turbulence can help us to interpret observations, which are incapable of fully resolving the space-time variability of naturally occurring turbulence. In this section, we survey some issues involved in computer simulation of ocean turbulence.

Flow simulation begins with the specification of a computational grid, a collection of points in space at which flow variables (velocity, temperature, etc.) are to be computed. A specified initial flow state is then "evolved" forward in time using discrete approximations to the equations of motion. Ideally, the grid contains enough points to fully resolve both the largest and the smallest eddies (i.e. the entire spectrum shown in figure 5). Such a computation is called a direct numerical simulation (DNS). An example of a

DNS is shown in figure 4. Unfortunately, this ideal is not easily achieved for many flows of interest, and less direct methods are often needed, as we now describe.

The tremendous range of scales present in ocean turbulence poses a challenge for computer simulations, since the memory needed is proportional to the cube of the ratio of largest to smallest scale. It is evident that direct simulation of many regimes of ocean turbulence will not be possible in the foreseeable future. Because of this, a major focus of turbulence research is the development of models that can approximate the effects of the smallest fluctuations, eliminating the need to resolve them explicitly. Simulations based on such techniques are referred to as large eddy simulations, or LES.

An example of ocean LES output is given in figure 11. The model covered a rectangular region, bordering the ocean surface, approximately 100m deep and 300m on each lateral side. The grid spacing was approximately 1m. The model was initialized with observed profiles of velocity, temperature and salinity and forced at the surface with realistic wind stress, heat flux and precipitation. LES modeling provides a picture of the spatial and temporal variability of currents and scalar fields that is far more comprehensive than can be obtained from observational measurements. These data allow calculation of property fluxes in the upper ocean, as well as detailed diagnosis of the physical mechanisms at work.
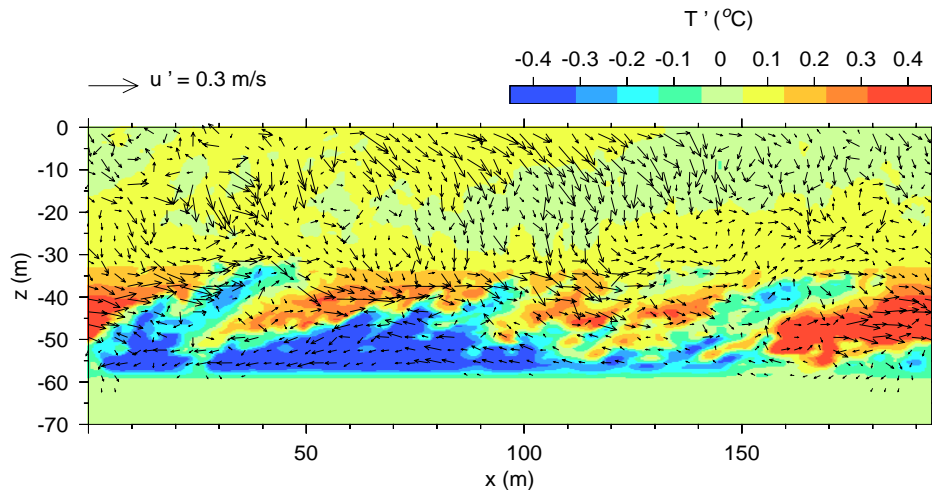

Figure 11: Cross-section of the upper ocean mixed layer during a storm, simulated using LES techniques. The x and z coordinates indicate downwind and vertical directions, respectively. Arrows show flow in the plane of the cross-section. Colors indicate the temperature anomaly, computed by subtracting the horizontally averaged profile (averaged over both x and y) from the temperature field. Red (blue) indicates regions in which the temperature is warmer (cooler) than the horizontally averaged value at that depth. This cross section represents a downwelling region, so that temperature anomalies tend to be positive.

The comprehensive information available from LES comes at a price: there is no guarantee that the model's behavior will match that of the ocean. Not only are the initial and boundary conditions approximate, the smallest scales of motion are not resolved explicitly. Unresolved scales (motions smaller than about 1m) generally include all of the dissipation range and some of the inertial range (figure 5). The

behavior of these unresolved scales is approximated by assuming that the turbulence is stationary, homogeneous and isotropic, and taking advantage of our theoretical understanding of that relatively simple case (section 3). As we have seen, however, these assumptions are of limited validity when applied to ocean turbulence (section 4).

Because of the uncertainties inherent in LES methods, it is important that we test models as thoroughly as possible by comparison with observational measurements. Results of such a comparison are shown in figure 12. Because of the chaotic nature of turbulence, we do not expect the model to reproduce the observations at each point in space and time; instead, we compare statistics taken over suitably chosen space-time intervals. For the case shown in figure 12, the statistics compared very well in the strongly turbulent region (-10m > z > -60m, the upper ocean mixed layer). In this region, the assumptions of stationarity, homogeneity and isotropy are relatively sound. In the strongly stratified region below z = -60m, turbulence becomes highly anisotropic (section 4.2), and model accuracy is reduced as a result. Near the surface (z > -10m) measurements are unavailable, but we expect turbulence to be anisotropic in that region due both to boundary proximity effects (section 4.3) and strong shear (section 4.1).

Figure 12: Comparison of ε statistics derived from LES (red) and oceanic measurements (blue). Histograms of modeled ε were compiled for several depth bins, describing both horizontal variability and evolution over an interval of two hours, and compared with measurements taken over the same time interval. The histograms corresponding to indicated depth ranges are shown in red; the observational measurements are shown in blue. Observations shallower than 10m are contaminated by ship wake and are thus discarded.
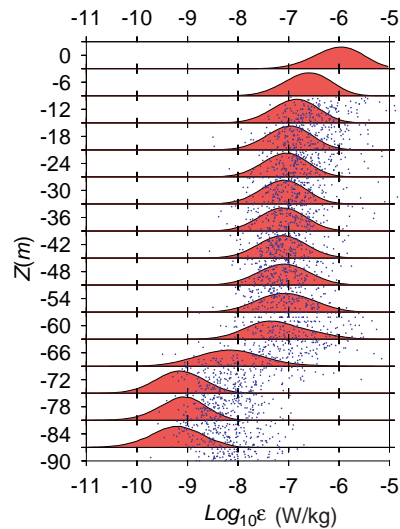
Large-scale ocean models employ grid resolution much coarser than LES, and the assumptions made in modeling the unresolved scales are correspondingly more tenuous. Nevertheless, such modeling efforts must be pursued as they provide our only access to crucial processes such as pollutant dispersal and anthropogenic climate change.

In summary, modeling techniques lead to significant new insights into the nature and role of turbulence in the oceans, but careful attention to the validity of the underlying assumptions is needed. As our understanding of real (i.e. nonstationary, inhomogeneous, anisotropic) turbulence improves, so will our ability to model ocean turbulence in all its complexity.

SUGGESTED READING

Frisch, U., 1995: *Turbulence*, 296 pp., Cambridge University Press, Cambridge

J.C.R. Hunt, O.M. Phillips and D. Williams, 1991: *Turbulence and stochastic processes;   Kolmogoroff's ideas 50 years on*, The Royal Society, London, 240 pp.

Kundu, P.K., 1990: *Fluid Mechanics*, 638 pp., Academic Press

KEY WORDS
turbulence, mixing, stratified flow, shear flow, boundary layers